An Effective Signal Processing Procedure for the Detection of Road Damages using Ground Penetrating Radar

A. BENEDETTO* F. BENEDETTO** M.R. DE BLASIIS* G. GIUNTA**
*Department of Science of Civil Engineering **Department of Electronic Engineering
University of ROMA TRE
Via della Vasca Navale 84, 00146 Rome
ITALY

Abstract: - Pavement damage is actually one of the most crucial problems in roads. Agencies need first to localize the damage, second to identify the causes. Indeed, the rehabilitation can be compromised, if the cause is not removed. The *ground penetrating radar* (GPR) technique is used by many agencies involved in roads management. In fact, it is nondestructive and is promising for soil characteristics interpretation, such as moisture or density. A preliminary detection and a subsequent classification of the pavement damage, based on an automatic GPR analysis, have been performed and experimentally validated. An optimum detection procedure is performed. It implements the classical Neyman-Pearson radar test, which is based on a constant false alarm rate strategy. All the setting needed by the optimum procedure have been estimated from a training set of measures. The overall performance has been evaluated by looking at the usual receiver's operating characteristic (ROC), obtained by processing a different (from the training phase) set of traces. The obtained results evidence that a reasonable performance has been achieved by a suited analysis of GPR images exploiting the spatio-temporal correlation properties of the received signal. Although a generalization is not reliable, this study shows that an automatic GPR-based evaluation of subgrade characteristics is feasible.

Key-Words: - Detection, Geophysical Signal Processing, Ground Penetrating Radar, Image Analysis, Spatio-temporal signal processing.

1 Introduction

Actually the pavement damages and defects so as the loss of mechanical properties in the subgrade [6] represent one of the most crucial problems in rehabilitation of roads [5]. Recent outcomes of relevant Italian research project [8] have shown that about 30% of road accidents, that happens on the national network, is caused by the pavement damages and defects. In Italy, so as in many other countries, the financial resources for the infrastructures management are very low. Therefore only a programmed plan, directed to remove the causes of the damages, can reach benefits. In this framework the *ground penetrating radar* (GPR) new technology seems to be very promising.
Usually it is easy to localize the damage [11]-[13], but it is always difficult to identify the specific causes, because they are frequently hidden in subgrade or under the ground layer. This lack of information can compromise the works for rehabilitation, because if the cause is not completely removed the effect occurs again.

The GPR technique is used by many Agencies involved in roads management [7],[10] to evaluate the layer thickness [3], anomaly location, such as the presence of voids or segregation [2] and to classify the type of media. The principal point of strength of this method is that it is nondestructive. Some experimental studies have shown the promising frontiers of GPR based analysis for soil characteristics, such as moisture content or density [1],[9].

2 Procedure description

The road is scanned in a sequence of vertical radar reflections. The vertical sweeps samples are regularly spaced. The proposed procedure considers the generic time delay (τ_i^j) of a radar signal, where (j) is the index of the longitudinal or transversal road scan sample and (i) is the index of the depth sample. The detection is based on a threshold analysis between the delay average ($<\tau_i>$), induced by a continuous interface of the layer (i), and the generic time delay (τ_i^j). If the difference between these two

delays is less than a minimum fixed threshold value (η) the layer is a horizontal straight outline. On the other hand, if the above-mentioned difference is greater than the adopted threshold value, the analysis yields the presence of a singularity:

$$\| < \tau_i > - \widehat{\tau_i^j} \| < \eta \quad \text{horizontal layer}$$
$$\| < \tau_i > - \widehat{\tau_i^j} \| > \eta \quad \text{singularity} \qquad (1)$$

If e is the error induced by the singularity, the delay can be expressed as:

$$\tau_i^{(j)} = \widehat{\tau_i^j} + e \qquad (2)$$

It is now possible to compare this stochastic variable e with a second threshold.

$$\| e \| > \lambda \quad \text{short wave length singularity}$$
$$\| e \| < \lambda \quad \text{long wave length singularity} \qquad (3)$$

where λ is the second threshold value.
In other words, if the difference between the delay of one radar signal and the delay of the following one is greater than the second fixed threshold value, the checked anomaly is a pointed singularity (short wave length singularity). Otherwise the anomaly can be modeled as a widespread depression (or raising) of the layers (long wave length singularity). This is because of a sharp variation of the delay is a localized break of the layer continuity, while a continuous delay variation derives from a regular wavelike shape of the layer interface.
The equations (1) and (3) can be written exploiting the spatio-temporal correlation properties of the received signal. For the first analysis, introducing two indexes N and M respectively related to the number of the analyzed radar sweeps (N) and to the dimension of a sliding window centered on the j trace (M), it is:

$$\left\| \frac{1}{N} \sum_{j=1}^{N} \tau_i^j - \frac{1}{M} \sum_{l=j-M/2}^{j+M/2} \tau_i^l \right\| \rightarrow \begin{cases} < \eta \\ \\ > \eta \end{cases} \qquad (4)$$

obviously, with $M << N$.
Likewise, for the second threshold analysis, it is:

$$\left\| \tau_i^j - \frac{1}{W} \sum_{l=j-W/2}^{j+W/2} \tau_i^l \right\| \rightarrow \begin{cases} < \lambda \\ \\ > \lambda \end{cases} \qquad (5)$$

where, similarly as before, $W << N$ is the second sliding window width.

3 Theoretic framework

The detection procedure implements the classical Neyman-Pearson radar test [14], which is based on a constant false alarm rate strategy. The test is a binary decision problem in which each of the two source outputs corresponds to a hypothesis. The two hypotheses are labelled as H_0 and H_1, and H_0 corresponds to the presence of no anomalies (horizontal layer) while H_1 indicates the presence of a singularity. If H_1 is true, then the second threshold analysis starts. This analysis is also based on the Neyman-Pearson test but now the two hypotheses are conditioned to H_1. In fact, H_{01} yields the presence of a long wave singularity while H_{11} corresponds to the presence of a short wave singularity. Each hypothesis maps into a point in the observation space corresponding to a set of N observation: r_1, r_2,…, r_N. Once the decision region Z_0 and Z_1 are chosen the values of the probabilities are determined [14]:

$$P_F = \int_{Z_1} p_{r|H_0}(R|H_0) dR \qquad (6)$$

$$P_D = \int_{Z_1} p_{r|H_1}(R|H_1) dR \qquad (7)$$

The subscripts are mnemonic and chosen from the radar problem in which H_1 corresponds to the presence of a target and H_0 to its absence. P_F is the probability of a false alarm (we say the anomaly is present when it's not) and P_D is the probability of detection (we say the anomaly is present when it is).
To complete our discussion we must evaluate the performance of the test. For a Neyman-Pearson test the values of the two conditioned probabilities P_F and P_D completely specify the test performance. We should like to make P_F as small as possible and P_D as large as possible. These are conflicting objectives, so an obvious criterion is to constrain one of the probabilities and maximize (or minimize) the other. If we constrain $P_F = \alpha' < \alpha$, the aim of the test is to maximize P_D. We obtain, for the first analysis:

$$P_F = p\left(\hat{H}_1 | H_0 \right) \qquad (8)$$

$$P_D = p\left(\hat{H}_1 | H_1 \right) \qquad (9)$$

For the second test we have:

$$P_F = p\left(\hat{H}_{11} \middle| H_1, H_{10} \right) \quad (10)$$

$$P_D = p\left(\hat{H}_{11} \middle| H_1, H_{11} \right) \quad (11)$$

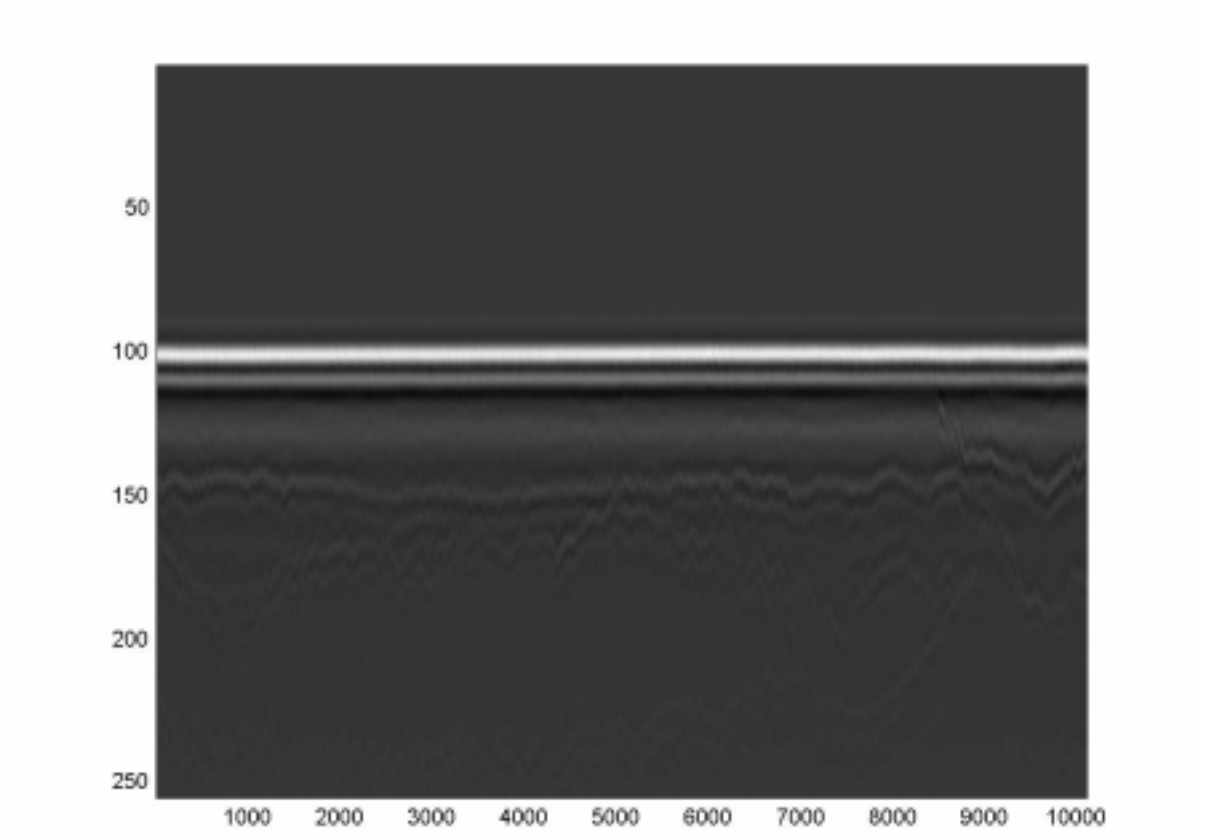

Figure 1. *Radar gram along the GRA road.*

4 Experimental results

An on road experimental survey is carried out to compute the performance of the test. This validation survey has been carried out on one exit of the ring highway of Rome (GRA – *Grande Raccordo Anulare*). Six longitudinal and six transversal scans (for total length about 1 km) have been performed. In particular we analyze a 100 m longitudinal scan with a subgrade depression located in the last 15 meters (fig. 1).

We evaluate the ROC (receiver operating characteristic), P_F on the horizontal axes and P_D. on the vertical axes, compared to the changing of the above-mentioned indexes. All the ROC must be above the $P_D = P_F$ line (bisector) and concave downward. If they were not, a randomized test would be better. Moreover the slope of a curve in a ROC at a particular point is equal to the value of the threshold required to achieve the P_D and P_F of that point. For the first test, fixing M=1 we obtain for N=500, 1000, 2000 the following graphs:

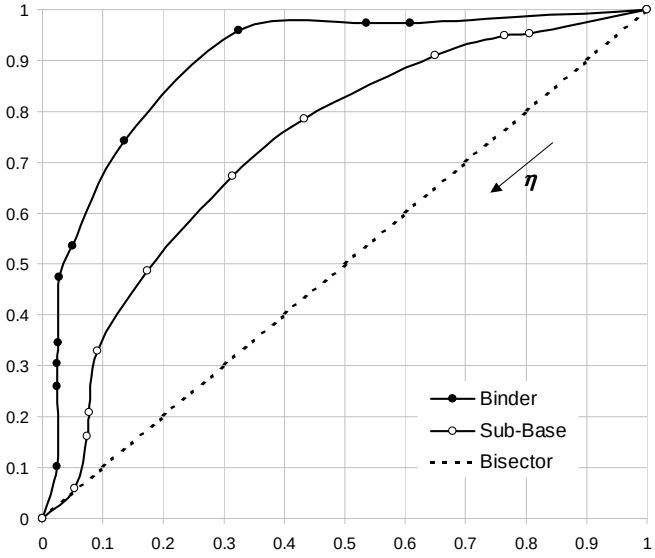

Figure 2. *ROC with N=500, M=1.*

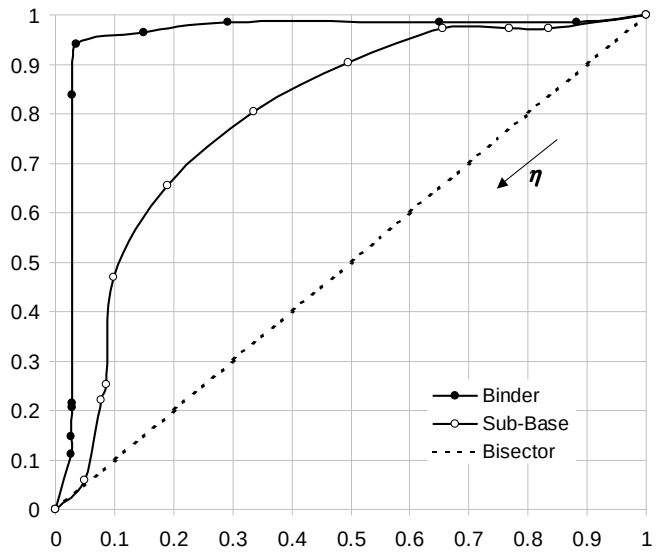

Figure 3. *ROC with N=1000, M=1.*

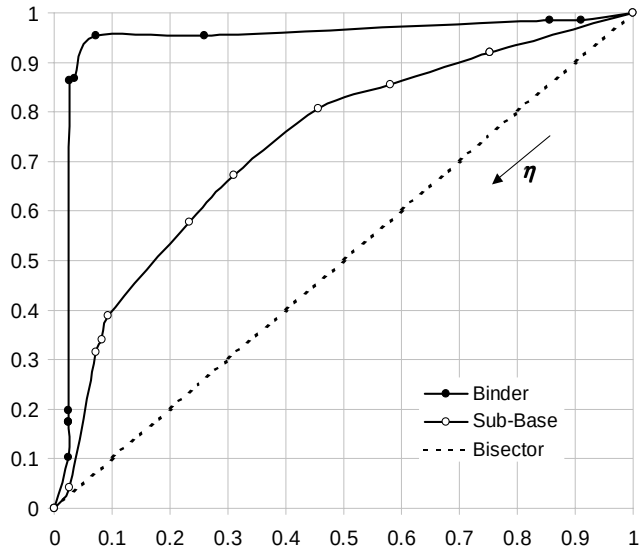

Figure 4. *ROC with N=2000, M=1.*

The best results can be achieved, both for the binder and the sub-base layers, with the first index N=1000. In fact with P_F =10% for the Binder layer and with P_F =20% for the Sub-Base layer, we obtain a probability of detection greater than 90% (for the binder) and greater than 70% (for the sub-base). The physical meaning of this behavior is discussed later. Moreover, we can try to improve these performance fixing the first index N=1000 and changing the width of the first sliding window. Exploiting the spatio-temporal correlation properties of the received signal, for N=1000 and M=3, 5 we have two new graphs (figures 5 and 6). After the detection of the anomalies, the second test for the classification of the damage itself starts. We can now evaluate the performance of this test, similarly of what we have done for the first analysis.

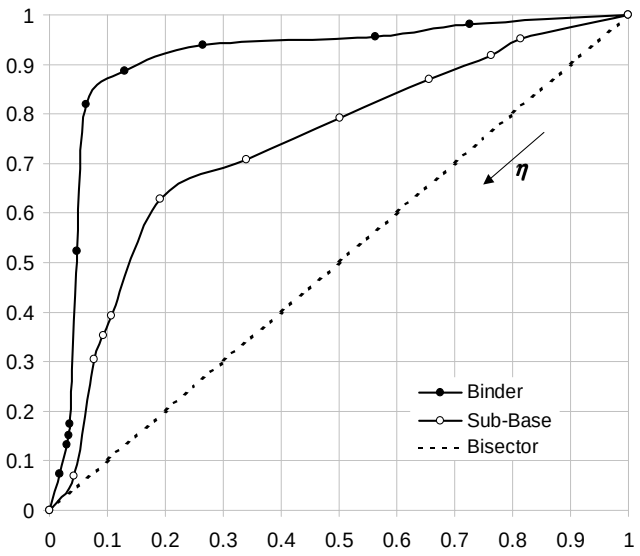

Figure 5. *ROC with N=1000, M=3.*

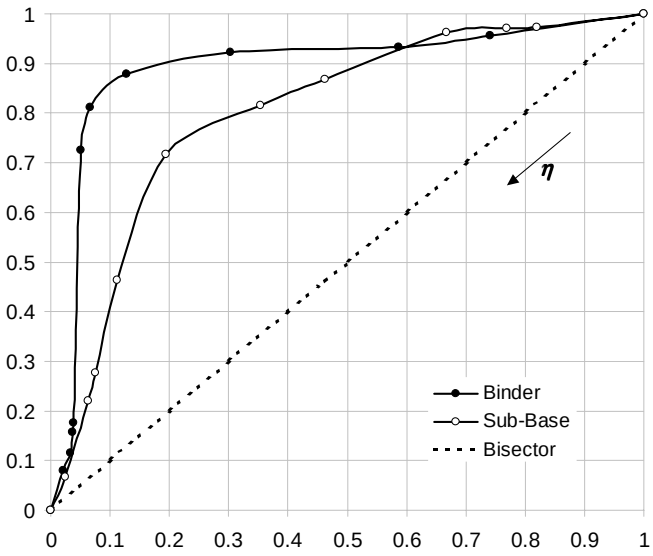

Figure 6. *ROC with N=1000, M=5.*

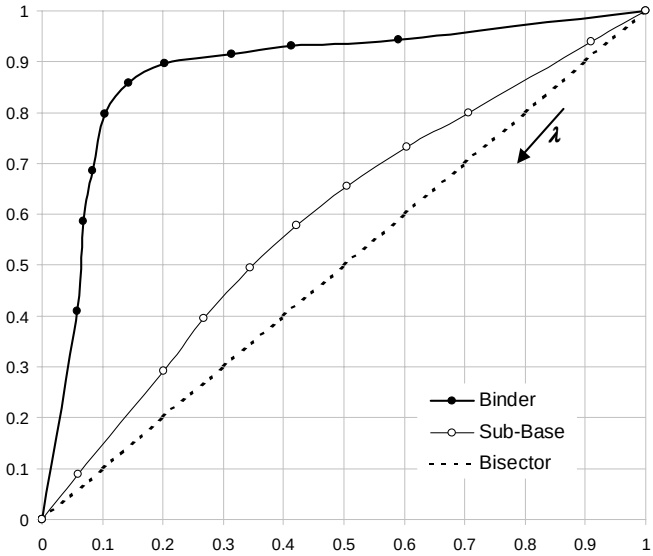

Figure 7. *ROC with W=25.*

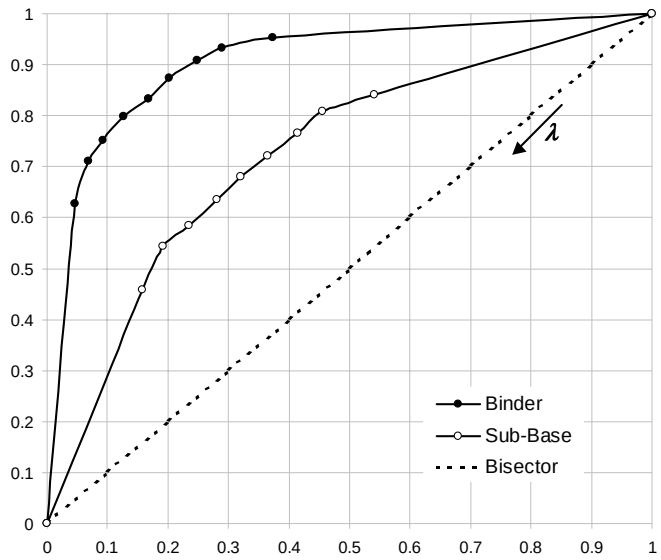

Figure 8. *ROC with W=9.*

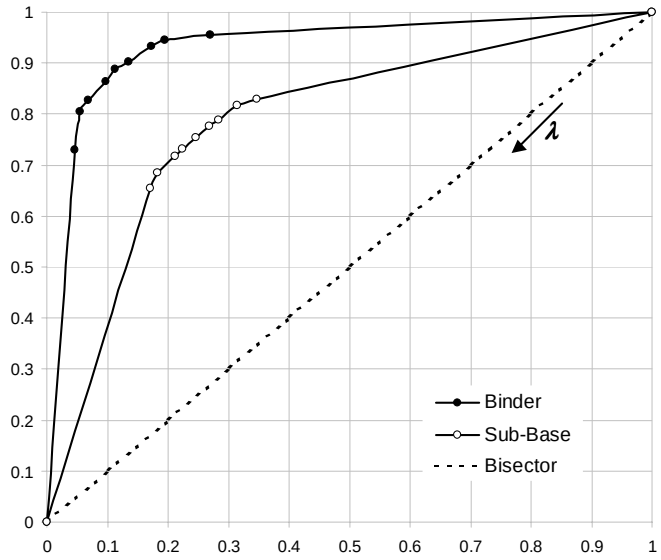

Figure 9. *ROC with W=5.*

Changing the width of the second sliding window W=25, 9, 5 we obtain the graphs illustrated in figures 7, 8 and 9. The meaning of these curves will be discussed below

5 Discussion

The outcomes show clearly the performance of the proposed procedure implemented with the two thresholds' analysis. Figures 2, 3 and 4, show the ROCs for the first test implemented with different values of the index N, that is the total number of the radar sweeps. The curves are sensible different because of the dimension of the analyzed anomaly itself. In fact, the sub-grade depression is localized in the last 15 meters of the road scan.

The use of N=500 (figure 2) means that the singularity lies too "heavy" on the estimate of the mean delay; on the other hand, the use of N=2000 (figure 4) means that the depression doesn't affect the estimate at all and it is not properly recognized from the algorithm. Instead, with N=1000 (figure 3), the automatic procedure is able to well detect the localized damage.

Figures 5 and 6 show the ROCs obtained with N=1000, the best case, while changing the spatio-temporal correlation between the radar sweeps. The curve of the binder layer doesn't need improving, in fact for P_F =10% we have P_D >90%. We concentrate our efforts to improve the values of the sub-base layer: with M=5, figure 6, we achieve an acceptable value of P_D (>70%) fixing P_F =20%.

For the second test the treatment is analogous. While the detected anomaly is a long wave singularity the best result can be achieved reducing the width of the spatio-temporal correlation (figures 7, 8 and 9). In fact smaller the sliding window width is, greater the achieved P_D.

Actually it is difficult to generalize a value of the two thresholds. Anyway the proposed algorithm seems to be very promising to identify hidden damage (fig. 6). If very low values for the η threshold, detection procedure, are assumed, the risk of ambiguities due to the super resolution of the algorithm rises, but if the value is too high the thin layers can not be solved. Usually the 0.5cm or less layers are unresolved [4]. Moreover, the survey shows that the second threshold analysis greatly depends on the characteristics of the damage itself. To identify a reasonable value for the λ threshold classification procedure, a wide on road investigation is needed. It means that the validation on road is of special importance.

6 Conclusion

The *ground penetrating radar* (GPR) technique has been used for the automatic detection and classification of roads' pavement damages. A preliminary detection and a subsequent classification of the pavement damage, based on an automatic GPR analysis, have been performed and experimentally validated.

An optimum detection procedure is performed. It implements the classical Neyman-Pearson radar test, which is based on a constant false alarm rate strategy. The obtained results evidence that a reasonable performance has been achieved by a suited analysis of GPR images exploiting the spatio-

temporal correlation properties of the received signal.

Acknowledgments

This work is based on the Master thesis in *Electronic Engineering* of Mr. F. Benedetto. The authors wish also to thank Prof. G. Schettini of *University of Roma Tre* that has contributed as *thesis' advisor*.

References

[1] Benedetto A., Benedetto F., (2002), GPR Experimental Evaluation of subgrade soil characteristics for rehabilitation of roads, *Proceedings of ninth International Conferences on GPR*, Santa Barbara, California, USA.

[2] Benedetto, A., De Blasiis M.R. (2001), Road pavement diagnosis, *Quarry and Construction*, **6**, 93-111.

[3] Davis, J.L., Rossiter J.R., Mesher D.E., Dawley C.B. (1994), Quantitative measurement of pavement structures using radar, *Proceedings of fifth International Conferences on GPR*, Kitchener, Ontario, Canada.

[4] Dérobert, X., Fauchard, C., Côte, Lebrusq, E., Guillanton, E., Dovignac, J.Y., Pichot (2001), Step-frequency radar applied on thin road layers, *Journal of applied Geophysics*, **47**, 317-325.

[5] Heiler, M., McNeil, S. (1997), Interpreting Ground Penetrating Radar Pavement Data, *Proc. of the ASCE Conf. Infrastructure Condition Assessment*, Boston, USA.

[6] Huston, D., Pelczarski, N., Esser, B., Maser, K. (2000), Damage detection in road ways with GPR, *Proc. VII International Conf. on GPR, Gold Coast, Australia.*

[7] Morey, R. (1998), Ground Penetrating Radar for evaluating subsurface conditions for transportation facilities, Synthesis of highway practice 255, National Cooperative Highway Research Program, TRB, National Academy Press.

[8] PRIN (1997-1999), Project standard of the infrastructures in function to the road induced visual information and the psychophysical stress, Ministry of University and Scientific Research, Italy.

[9] Saarenketo, T (1998) Electrical properties of water in clay and silty soils, *Journal of Applied Geophysics*, **40**, 73–88.

[10] Saarenketo, T., Scullion T. (2000), Road evaluation with ground penetrating radar, *Journal of Applied Geophysics*, **43**, 119–138.

[11] SETRA, LCPC (1979) Entretien préventif du réseau routier national.

[12] SHRP National Research Council (1993) Distress identification manual for the long-term pavement performance project.

[13] VSS Norme Suisse (1991) Catalogue des dégradations.

[14] H.L. Van Trees, "Detection, Estimation, and Modulation Theory", New York: *Wiley*, 1971.